Adaptive control of a two-stage vibration isolation mount

Scott D. Sommerfeldt and Jiri Tichy
Applied Research Laboratory and Graduate Program in Acoustics, The Pennsylvania State University, P. O. Box 30, State College, Pennsylvania 16804

(Received 16 November 1989; accepted for publication 2 March 1990)

An adaptive control system has been developed that may be used for active noise and vibration control problems involving one-dimensional propagation. Based on the least-mean-squares (LMS) algorithm, the adaptive controller performs both system identification and control in real time, without the need for *a priori* measurements of the system. Since the controller is adaptive in nature, it is possible to track changes in the system while maintaining optimal control. In the present application, the adaptive control system was applied to the problem of minimizing the force transmitted through a two-stage vibration isolation mount. The control system was implemented in real time using a Motorola DSP56000ADS signal-processing board and applied on a physical vibration isolation mount. For periodic excitations, the adaptive controller was capable of providing 30- to 40-dB attenuation of the transmitted vibration. For broadband excitation, some limitations exist, but the controller was still capable of providing about 20-dB attenuation over the lower frequency range. The controller also demonstrated the ability to track changing system parameters to maintain optimal control of the system.

PACS numbers: 43.40.Vn

INTRODUCTION

There are numerous practical applications where it is desired to isolate a vibrating structure from surrounding structures, as a means of minimizing the vibration which is transmitted away from the vibrating structure. In the case of vibrating engines, generators, and other such structures, vibration isolation mounts have typically been used to isolate the structure from the foundation on which it is mounted. Various types of isolation mounts have been devised to achieve particular frequency response characteristics. However, one feature common with all of these passive mounting schemes is that the transmissibility associated with the mount is significantly higher in the low-frequency region than in the high-frequency region.

In recent years, active control has been investigated as a possible solution to attain greater transmission loss in the low-frequency region of isolation mounts.[1–3] Active control involves the application of "secondary" forces to the system to cancel (or reduce) the forces generated by the "primary" source. Since this technique involves superposition of forces, active control tends to be most effective at lower frequencies, where the amplitude and phase of the interacting forces can be accurately matched with minimal error. Given that active control is most effective at lower frequencies, one solution to the isolation problem would be to combine an active force controller with a passive mounting system. Such an approach would provide good attenuation in both the low- and high-frequency regions.

Typically, active controllers have been developed based on a model of the system (structure) to be controlled.[4–7] As such, they will provide optimal control as long as the model accurately represents the system. However, if the model is inaccurate, or if the parameters of the system change, the active controller may result in suboptimal control. Particularly for complex structures, it may be a significant task to obtain a sufficiently accurate model of the system to develop the optimal controller, and the model is only good as long as the system parameters do not change.

Adaptive control provides an attractive means of implementing active control. Since the control algorithm is adaptive, it is not as critical to have an accurate model of the system to be controlled. The adaptive controller will learn the characteristics of the system and converge to the optimal controller for the current parameters and control filter structure. In addition, if the parameters of the system change in real time, the adaptive controller has the ability to track those changes.

Adaptive control has been applied to a number of problems involving the reduction of air-borne noise. Many of the successful applications to date have involved the reduction of noise in ducts.[8–10] This problem involves one-dimensional wave propagation and represents a simpler system to be controlled than the more general case of three-dimensional propagation. Recently, work has also been progressing on the three-dimensional propagation problem.[11,12]

The adaptive algorithms that have been developed for control applications can be grouped into two general categories: least-squares algorithms and steepest-descent-type algorithms. The most popular algorithm that has been used for adaptive noise and vibration control is a steepest-descent-type algorithm, referred to as the least-mean-squares (LMS) algorithm. The LMS algorithm was developed by Widrow *et al.*[13–15] for use in signal-processing applications and is noted for its simplicity in implementation.

This paper reports the development of an adaptive vibration controller, briefly reported previously,[16] which is based on the LMS algorithm. The controller has been applied to a two-stage vibration isolation mount. This structure involves one-dimensional motion and represents the structural analog of the duct problem mentioned previously. For the adaptive controller to converge properly, it is necessary

 © 1990 Acoustical Society of America

Redistribution subject to ASA license or copyright; see http://acousticalsociety.org/content/terms. Download to IP: 128.187.97.22 On: Tue, 01 Apr 2014 19:15:00

to know the transfer function between the controller and the "error" signal. The error signal provides information regarding the effectiveness of the controller. The determination of this transfer function is referred to as "system identification." The adaptive controller described here performs system identification and control simultaneously in real time to provide optimal control of the system.

I. DEVELOPMENT OF THE ALGORITHM

For an adaptive controller based on the LMS algorithm, the control signal is obtained as the convolution of the input data to the controller with the control filter coefficients. Thus the control signal $y(t)$ can be written as

$$y(t) = \sum_{i=0}^{I-1} w_i(t)x(t-i), \tag{1}$$

where $x(t)$ is the input data sequence, and $w_i(t)$ represents the LMS filter coefficients, which may be time varying. The control signal $y(t)$ is applied to the system via some "secondary" control actuator in an attempt to achieve some desired response from the system. (In the context of this paper, the system consists of the two-stage vibration isolation mount, and the desired response is zero transmitted force.) The difference between the measured response and the desired response represents a measure of the error in controlling the system, and can be used to adapt the controller to achieve optimal control, as will be shown shortly. Thus the task of the controller is to determine the filter coefficients $w_i(t)$ that will give the optimal control sequence $y(t)$, which minimizes the error.

In the context of adaptive noise or vibration control, a transfer function exists that relates the control filter output $y(t)$ to the response of the system to that control at the error sensor. This is shown schematically in Fig. 1, with H representing this transfer function. For the problem considered here, this transfer function represents the D/A convertor, the control actuator, the system between the control actuator and error sensor, and the error sensor. The approach developed in this paper uses the assumption that this transfer function can be sufficiently accurately modeled by a finite-impulse-response (FIR) filter. Using this assumption, the response of the system measured by the error sensor can be written as

$$e(t) = d(t) + \sum_{j=0}^{J-1} h_j(t)y(t-j), \tag{2}$$

where $e(t)$ is the measured error sensor data sequence, $d(t)$ is the response of the system to the "primary" input and represents the signal to be canceled, and the $h_j(t)$ represent the transfer function from the controller output to the error sensor and may be time varying. For proper convergence of the controller, it is necessary to know the transfer function associated with $h_j(t)$. This represents a problem of system identification and is an issue that has been addressed by a number of researchers. Burgess[17] discussed the need to have a knowledge of the transfer function H to ensure proper convergence. Since then, a number of methods have been developed to obtain H. Warnaka *et al.*[9] developed an off-line approach that compensated for H by introducing a secondary "compensation" filter in series with H, which was adaptively set to equal the inverse of H within a pure delay. Thus the overall error path transfer function appears as z^{-d}, where d is the delay associated with H. Widrow and Stearns[18] developed what is known as the "filtered-x" algorithm, which incorporates a fixed model of H into the development of the control algorithm. This results in a modified LMS-type adaptive algorithm. Eriksson and Allie[19] developed an on-line approach that estimates H through use of a random noise sequence which is injected into the system. Stability issues related to these various approaches have been investigated by Ren and Kumar.[20] The approach developed in this paper is closely related to the filtered-x algorithm of Widrow and Stearns.

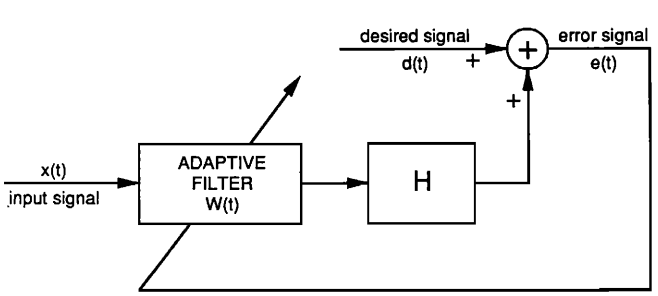

FIG. 1. Block diagram showing generalized control scheme.

Using Eq. (1) allows Eq. (2) to be written as

$$e(t) = d(t) + \sum_{j=0}^{J-1} h_j(t) \sum_{i=0}^{I-1} w_i(t-j)x(t-j-i). \tag{3}$$

The task of the adaptive controller involves both system identification and control. The system identification involves identifying the proper values for the $h_j(t)$, while the control involves identifying the proper values for the $w_i(t)$. One or the other, or both of these tasks can be performed off-line to develop an active controller. However, the resulting controller will only be optimal as long as the parameters estimated off-line do not change in real time. Alternatively, both of these tasks can be performed adaptively in real time, as will be shown presently.

A. System identification

For an LMS-based control system, the signal to be canceled, $d(t)$, is assumed to be correlated with the input signal to the controller, $x(t)$. Representing this relationship with an FIR filter allows $d(t)$ to be expressed as

$$d(t) = \sum_{k=0}^{K-1} c_k(t)x(t-k), \tag{4}$$

where the coefficients $c_k(t)$ represent the transfer function from the input $x(t)$ to the response $d(t)$. For the development to follow, it will be convenient to introduce vector notation. Accordingly, define

$$\mathbf{\Theta}^T(t) \equiv [h_0(t)h_1(t)\cdots h_{J-1}(t)c_0(t)c_1(t)\cdots c_{K-1}(t)], \tag{5}$$

$$\mathbf{\Phi}^T(t) \equiv [y(t)y(t-1)\cdots y(t-J+1)x(t) \cdots x(t-K+1)]. \tag{6}$$

These definitions allow the error signal in Eq. (2) to be represented as

Redistribution subject to ASA license or copyright; see http://acousticalsociety.org/content/terms. Download to IP: 128.187.97.22 On: Tue, 01 Apr 2014 19:15:00

$$e(t) = \mathbf{\Theta}^T(t)\mathbf{\Phi}(t). \tag{7}$$

All of the values in $\mathbf{\Phi}(t)$ are available, either as measured or calculated data, as is the value of $e(t)$. The only values not available are the coefficients in $\mathbf{\Theta}(t)$, which are to be estimated. Equation (7) is in the form used to develop a number of adaptive algorithms for estimating $\mathbf{\Theta}(t)$. The projection algorithm[21] (also referred to as the normalized LMS algorithm) was chosen to provide this estimate in the present application. For the projection algorithm, the estimate of the coefficient vector $\hat{\mathbf{\Theta}}(t)$ is updated in a recursive manner, according to

$$\hat{\mathbf{\Theta}}(t+1) = \hat{\mathbf{\Theta}}(t) + \frac{a\mathbf{\Phi}(t)}{b + \mathbf{\Phi}^T(t)\mathbf{\Phi}(t)} \times [e(t) - \hat{\mathbf{\Theta}}^T(t)\mathbf{\Phi}(t)]. \tag{8}$$

In this expression, the term $\mathbf{\Phi}^T(t)\mathbf{\Phi}(t)$ has the effect of normalizing the update term by the power of the data sequence. The constant b is chosen to be some small, positive value to prevent division by 0, and the value of a controls the step size of the algorithm. To ensure convergence, a must satisfy $0 < a < 2$. Equation (8) is obtained by minimizing the cost function given by

$$J = \tfrac{1}{2}E\{[\hat{\mathbf{\Theta}}^T(t) - \hat{\mathbf{\Theta}}^T(t-1)]^2\}, \tag{9}$$

subject to the constraint

$$e(t) = \hat{\mathbf{\Theta}}^T(t)\mathbf{\Phi}(t). \tag{10}$$

Here, $E\{\cdot\}$ denotes the expectation operator. A geometric interpretation is that the present estimate of $\hat{\mathbf{\Theta}}(t)$ consists of the orthogonal projection of the previous estimate onto the present data space. The solution for $\mathbf{\Theta}^T(t)$ is not necessarily unique, as this property depends on the properties of the input data.[22] However, even if the solution is nonunique, the algorithm will converge to a solution that minimizes the difference between the measured error signal $e(t)$ and the estimated error signal $\hat{\mathbf{\Theta}}^T(t)\mathbf{\Phi}(t)$. This convergence property is sufficient for adaptive noise and vibration control applications, since the true value of $\mathbf{\Theta}(t)$ does not necessarily need to be known.

B. LMS control filter

To determine the algorithm for computing the optimal LMS control filter coefficients, it is useful to consider the case in which the filter coefficients w_i are time invariant. This is approximately the case after the filter has converged close to its steady-state value. With w_i time invariant, the approach developed by Elliott *et al.*[23] can be followed, in which Eq. (3) is rearranged as

$$e(t) = d(t) + \sum_{i=0}^{I-1} w_i \sum_{j=0}^{J-1} h_j(t)x(t-j-i). \tag{11}$$

This equation can be simplified by defining

$$r(t-i) \equiv \sum_{j=0}^{J-1} h_j(t)x(t-i-j). \tag{12}$$

The quantity $r(t)$ can be viewed as a filtered version of the input signal and, in essence, corresponds to inverting the order of the control loop transfer function $h_j(t)$ and the LMS control filter transfer function w_i. Returning to vector notation, define

$$\mathbf{W}^T(t) \equiv [w_0 w_1 \cdots w_{I-1}], \tag{13}$$

$$\mathbf{r}^T(t) \equiv [r(t)r(t-1)\cdots r(t-I+1)]. \tag{14}$$

With these definitions, the error signal can be written as

$$e(t) = d(t) + \mathbf{W}^T\mathbf{r}(t). \tag{15}$$

The LMS algorithm results from minimizing the performance criterion J, given by

$$J = E\{e^2(t)\}. \tag{16}$$

This minimum can be obtained by taking the gradient of J with respect to W and equating the result to zero. However, the expected values required in this process are generally not available, and some sort of estimate must be used. The estimate that LMS-based algorithms use is the gradient of the instantaneous squared error. The filter coefficients are updated recursively, using the negative of the gradient estimate, with the objective of converging to the optimal solution along a path close to the path of steepest descent. Denoting the estimate by $\hat{\nabla}_W J$, and using Eq. (15),

$$\hat{\nabla}_W J = \nabla e^2(t) = 2e(t)\mathbf{r}(t). \tag{17}$$

The update equation for the LMS control filter coefficients can now be written as

$$\mathbf{W}(t+1) = \mathbf{W}(t) - \mu e(t)\mathbf{r}(t), \tag{18}$$

where μ is a convergence parameter greater than zero, chosen to maintain stability. As well, the factor of 2 in Eq. (17) has been absorbed into the value for μ. It can be shown[24] that the algorithm described by Eq. (18) is stable for $0 < \mu < 2/\lambda_{\max}$, where $\lambda_{\max}$ is the largest eigenvalue of the matrix $E[\mathbf{r}^T(t)\mathbf{r}(t)]$. In practice, $\lambda_{\max}$ is generally not known. However, a more restrictive convergence region can be developed based on the average input signal power, which is useful for implementing the algorithm.[25] The resulting expression is given by

$$0 < \mu < 2/h_{\max}^2 (I \cdot J^2) R_{xx}(0), \tag{19}$$

where $R_{xx}(0)$ is the average input signal power, and $h_{\max}$ is the largest value the $h_j(t)$ assume.

Equations (1), (8), (12), and (18) comprise the equations that are implemented by the adaptive controller to simultaneously perform system identification and control in real time. The form of the control system corresponds to the filtered-x LMS algorithm of Widrow and Stearns,[18] the primary difference being that the filtered-x LMS algorithm does not perform the system identification task.

II. EXPERIMENTAL APPARATUS

The control system described in the previous section was implemented in real time using the Motorola DSP56000ADS signal-processing board, in conjunction with the Ariel ADC56000 I/O board. In the present application, the controller was used to provide adaptive vibration control for a system consisting of a single two-stage vibration isolation mount (Fig. 2). A two-stage isolation mount consists of a primary mass M_1 mounted on a spring–mass–spring system (k_1^*–M_2–k_2^*) to provide isolation from the

Redistribution subject to ASA license or copyright; see http://acousticalsociety.org/content/terms. Download to IP: 128.187.97.22 On: Tue, 01 Apr 2014 19:15:00

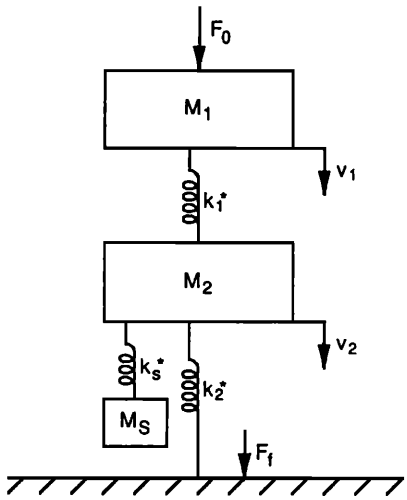

FIG. 2. Two-stage isolation mount with control force actuator attached.

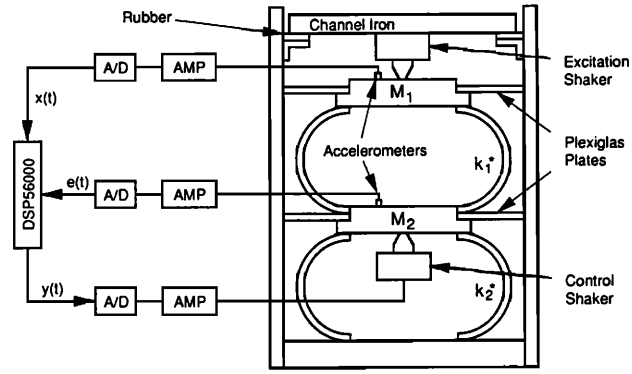

FIG. 3. Schematic diagram of the two-stage isolation mount.

foundation. (Asterisks denote complex quantities to include any losses in the system.) Such a mount is attractive as a passive mount, producing a roll-off in transmissibility of 24 dB/oct in the high-frequency range.[26] The disadvantage of such a mount is that it becomes ineffective in the low-frequency range. There are two resonances associated with the two degrees of freedom for the system. At these resonances, there is actually an amplification of the force transmissibility. As well, even at nonresonance frequencies in the low-frequency range, there is little or no attenuation of the transmissibility. By combining an active controller with the two-stage mount, it is possible to achieve good attenuation in both frequency ranges.

The objective for the present application is to minimize the transmission of forces generated in M_1 to the foundation. It was decided to provide the active control by means of an electrodynamic shaker (Wilcoxon F4) suspended from the intermediate mass M_2. This provides an inertial control force that may be applied to M_2 without creating a second force transmission path. Using this type of control also increases the degrees of freedom in the system by one. As a result, three resonances now exist in the low-frequency region, as well as an antiresonance at the resonance frequency of the shaker. At this frequency, the shaker behaves as a passive dynamic absorber to reduce the transmissibility. The setup is shown in Fig. 3. A second shaker is attached to M_1 to excite the system, thereby simulating the generation of forces that might occur in practice. The input and error signals were obtained by means of PCB 303A11 accelerometers, mounted on M_1 and M_2, respectively. In the present application, the acceleration of M_2 can be used as the error signal, since the transmitted force is proportional to the displacement (and hence the acceleration) of M_2 for a rigid foundation, as assumed here.

The Plexiglas plates shown in Fig. 3 are used to limit the motion to the vertical direction. The plates are flexible, thereby presenting a low impedance in the vertical direction at low frequencies. However, they are very stiff in the horizontal direction, thereby minimizing any lateral or rocking motion. The springs for the mount consisted of semicircular rings, as depicted in Fig. 3. Such rings have been shown to have a linear stiffness characteristic for small-amplitude vibration[27] and were chosen since they support primarily bending-wave propagation. The reason this property is desirable will become apparent in the next section.

As mentioned, the objective in the control scheme was to minimize the force transmitted to the foundation. However, since the foundation is assumed rigid in the present application, the force at the foundation is proportional to the displacement of the secondary mass M_2 via the spring constant k_2^*. Thus minimizing the acceleration of M_2, obtained from the error accelerometer, is equivalent to minimizing the transmitted force. Therefore, the signal obtained from the error accelerometer can be used as a direct measure of the error in controlling the system.

III. EXPERIMENTAL RESULTS

The simplest control problem involves the attenuation of a single sinusoidal excitation signal. In this case, the controller only needs to determine the optimal amplitude and phase at a single frequency. Figure 4 shows a time history of the error signal amplitude for a 50-Hz excitation signal, using the controller described previously. For this particular example, the convergence time is about 700 ms. It should be mentioned that no attempt was made to match the optimal filter *a priori*. In fact, all LMS filter coefficients were initialized to zero. If an *a priori* estimate had been used, the convergence time for the error signal would be reduced significantly. The effectiveness of the controller can be more accurately assessed in the frequency domain. Figure 5 shows the error signal spectrum for the 50-Hz excitation signal, both before and after the controller has been turned on. For this case, the controller was able to provide about 39-dB attenuation of the error signal. A higher excitation frequency is shown in Fig. 6 (142.5 Hz), with a resulting attenuation of about 40 dB. Throughout the frequency region tested (up to 200 Hz), the controller was capable of providing about 30- to 40-dB attenuation for a sinusoidal excitation.

The controller is capable of operating on multiple-frequency components. Figure 7 shows the results for a multiple-frequency excitation signal, consisting of a 60-Hz sine wave and a 95-Hz sine wave. Both frequency components were attenuated by about 30 dB.

Redistribution subject to ASA license or copyright; see http://acousticalsociety.org/content/terms. Download to IP: 128.187.97.22 On: Tue, 01 Apr 2014 19:15:00

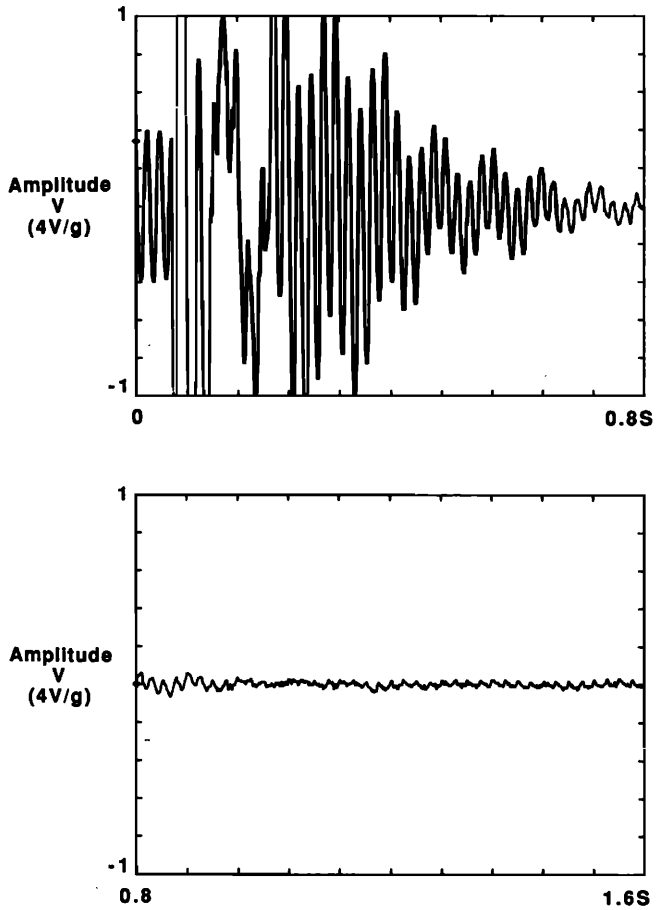

FIG. 4. Time history of the error signal—50-Hz excitation signal. (Control begins at about 55 ms.)

The controller was also tested using a broadband excitation signal, which consisted of white noise bandlimited to frequencies below 200 Hz (Fig. 8). The controller effectively attenuated the peak around 40 Hz by about 20 dB. However, for the peaks at lower and higher frequencies, very little attenuation was achieved. The lower peak around 20 Hz was not attenuated since the control shaker used was unable to generate any significant forces below about 30 Hz. To explain the response at higher frequencies, the phase-speed

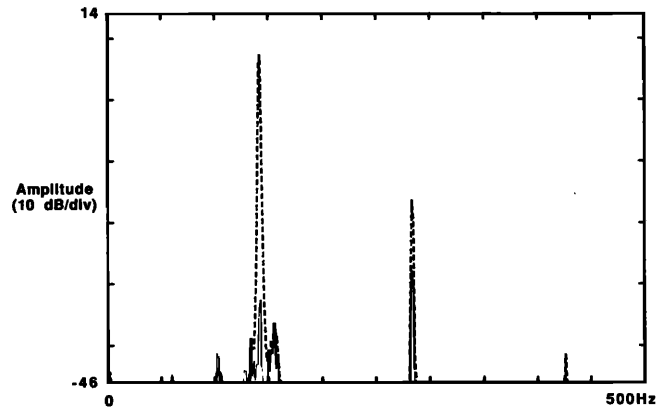

FIG. 6. Error signal spectrum—142.5-Hz excitation signal: without control, dashed line (7.2 dB); with control, solid line (− 32.6 dB).

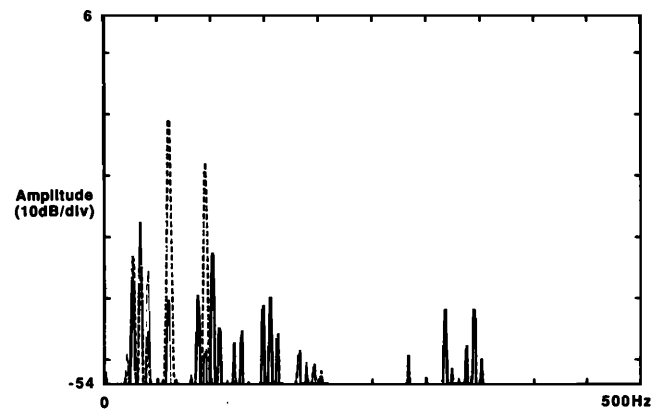

FIG. 7. Error signal spectrum—multiple frequency (60 and 95 Hz) excitation signal: without control, dashed line (− 11.2 dB, − 17.9 dB); with control, solid line (− 40.1 dB, − 48.2 dB).

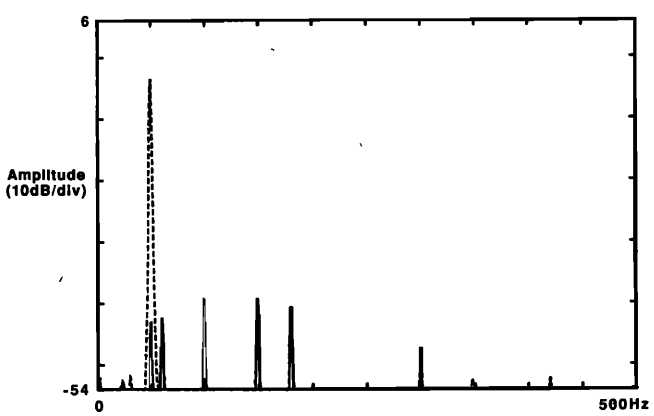

FIG. 5. Error signal spectrum—50-Hz excitation signal: without control, dashed line (− 3.6 dB); with control, solid line (− 43.0 dB).

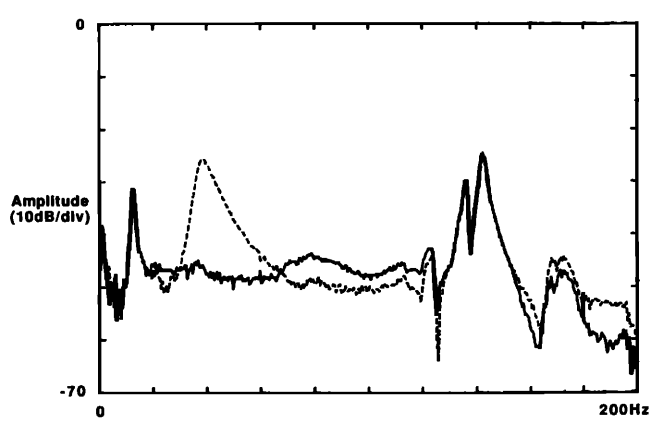

FIG. 8. Error signal spectrum—random excitation signal: without control, dashed line; with control, solid line.

Redistribution subject to ASA license or copyright; see http://acousticalsociety.org/content/terms. Download to IP: 128.187.97.22 On: Tue, 01 Apr 2014 19:15:00

characteristics of the system must be considered. For the control algorithm to provide effective control, the filtered input signal $\mathbf{r}(t)$ and the signal to be canceled $d(t)$ must be correlated, since the optimal control filter is proportional to the expected value of their product [Eqs. (15) and (16)]. For a random excitation signal, this means that the signal from the controller output must propagate to the error sensor at least as fast as the excitation propagates through the isolation mount to the error sensor. The delay through the control loop is relatively frequency independent, but the delay through the mount decreases according to the square root of increasing frequency, since the springs were designed to support primarily bending waves. Thus there exists a frequency where the delays through the two paths are equal, above which the delay through the mount is less than the delay through the control loop, and the two signals begin to become decorrelated. For the parameters associated with the two-stage mount used, it can be shown that the frequency where the two delays are equal is about 110 Hz.[28] This explains why there is relatively little attenuation in the 150-Hz region. It should be mentioned that this frequency limitation does not apply to periodic signals (Fig. 6), since $\mathbf{r}(t)$ and $d(t)$ remain correlated at all frequencies for periodic signals. The implication of this result is that the passive design of the system should be such that all significant resonances lie below the frequency limit of broadband control if a broadband input excitation is anticipated.

In addition, the controller was tested to determine its ability to track changes in the system parameters. The mount was designed to allow the mass of M_1 and M_2 to be gradually changed. In situations where one of these masses was gradually changed (by about 30% over a time frame of about 2 s), there was no perceptible change in the controlled error signal level. The system was also tested using an "impulsive" change in the mass. Figure 9 shows the case where the mass of M_2 was doubled. The impulse from introducing the mass can be observed, followed by a recovery time of about 20–30 ms.

IV. CONCLUSIONS

A generalization of the filtered-x LMS algorithm has been developed that performs both system identification and active control in real time. For the experimental setup used, the controller was very effective in providing active attenuation of periodic signals. The results for a broadband excitation indicate a deficiency at higher frequencies, as a result of the higher phase speed of propagation through the isolation mount. This deficiency would not exist for a system such as an air-filled duct and could be minimized for structural vibration through proper design of the system. The controller has proven to be robust with respect to changes in the system or changes in the input to the system.

The control system developed can be generalized to multiple-input/multiple-output problems to provide a method of achieving active noise or vibration control for systems involving multidimensional propagation.

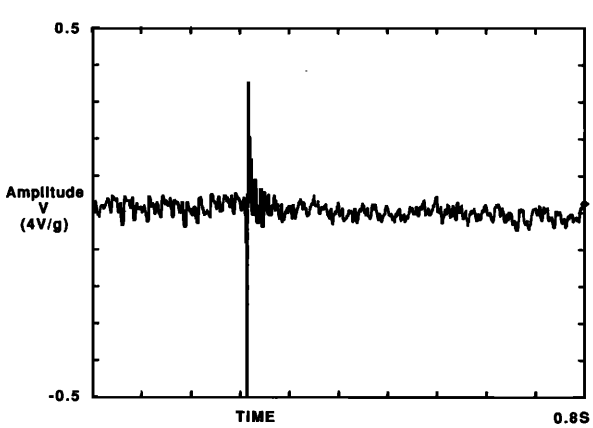

FIG. 9. Error signal waveform corresponding to doubling the mass M_2. (Uncontrolled amplitude of the error signal was ± 0.38 V.)

[1] S. Lee and A. Sinha, "Design of an active vibration absorber," J. Sound Vib. **109**, 347–352 (1986).

[2] J. S. Burdess and A. V. Metcalfe, "The active control of forced vibration produced by arbitrary disturbances," J. Vib. Acoust. Stress Reliability Design **107**, 33–37 (1985).

[3] T. Takagami and Y. Jimbo, "Study of an active vibration isolation system—A learning control method," J. Low Freq. Noise Vib. **4**, 104–119 (1985).

[4] L. Meirovitch, H. F. VanLandingham, and H. Öz, "Distributed control of spinning flexible spacecraft," J. Guidance Control **2**, 407–415 (1979).

[5] H. Öz and L. Meirovitch, "Optimal modal-space control of flexible gyroscopic systems," J. Guidance Control **3**, 218–226 (1980).

[6] L. Meirovitch and H. Baruh, "Optimal control of damped flexible gyroscopic systems," J. Guidance Control **4**, 157–163 (1981).

[7] C. R. Burrows and M. N. Sahinkaya, "Vibration control of multi-mode rotor-bearing systems," Proc. R. Soc. London Ser. A **386**, 77–94 (1983).

[8] L. A. Poole, G. E. Warnaka, and R. C. Cutter, "The implementation of digital filters using a modified Widrow–Hoff algorithm for the adaptive cancellation of acoustic noise," in *Proceedings of the 1984 IEEE International Conference on Acoustics, Speech, & Signal Processing* (IEEE, San Diego, 1984), Vol. 2, pp. 21.7.1–21.7.4.

[9] G. E. Warnaka, L. A. Poole, and J. Tichy, U. S. Patent 4,473,906 (1984).

[10] L. J. Eriksson, M. C. Allie, and R. A. Greiner, "The selection and application of an IIR adaptive filter for use in active sound attenuation," IEEE Trans. Acoust. Speech Signal Process. **ASSP-35**, 433–437 (1987).

[11] P. A. Nelson, A. R. D. Curtis, S. J. Elliott, and A. J. Bullmore, "The active minimisation of harmonic enclosed sound fields Parts I–III," J. Sound Vib. **117**, 1–58 (1987).

[12] J. V. Warner, D. E. Waters, and R. J. Bernhard, "Adaptive active noise control in three dimensional enclosures," in Proceedings of Noise-Con 88, June 1988, pp. 285–290.

[13] B. Widrow, J. R. Glover, Jr., J. M. McCool, J. Kaunitz, C. S. Williams, R. H. Hearn, J. R. Zeidler, E. Dong, Jr., and R. C. Goodlin, "Adaptive noise cancelling: Principles and applications," Proc. IEEE **63**, 1692–1716 (1975).

[14] B. Widrow, J. M. McCool, M. G. Larimore, and C. R. Johnson, Jr., "Stationary and nonstationary learning characteristics of the LMS adaptive filter," Proc. IEEE **64**, 1151–1162 (1976).

[15] B. Widrow and S. D. Stearns, *Adaptive Signal Processing* (Prentice-Hall, Englewood Cliffs, NJ, 1985), pp. 99–116.

[16] S. D. Sommerfeldt and J. Tichy, "Adaptive vibration control using an LMS-based control algorithm," in Proceedings of Inter-Noise 89, December 1989, pp. 513–518.

[17] J. C. Burgess, "Active adaptive sound control in a duct: A computer simulation," J. Acoust. Soc. Am. **70**, 715–726 (1981).

[18] B. Widrow and S. D. Stearns, *Adaptive Signal Processing* (Prentice-Hall, Englewood Cliffs, NJ, 1985), pp. 288–294.

[19] L. J. Eriksson and M. C. Allie, "Use of random noise for on-line transducer modeling in an adaptive active attenuation system," J. Acoust. Soc. Am. **85**, 797–802 (1989).

[20] W. Ren and P. R. Kumar, "Adaptive active noise control: Structures,

Redistribution subject to ASA license or copyright; see http://acousticalsociety.org/content/terms. Download to IP: 128.187.97.22 On: Tue, 01 Apr 2014 19:15:00

algorithms and convergence analysis," in Proceedings of Inter-Noise 89, December 1989, pp. 435–440.
[21] G. C. Goodwin and K. S. Sin, *Adaptive Filtering Prediction and Control* (Prentice-Hall, Englewood Cliffs, NJ, 1984), pp. 50–57.
[22] G. C. Goodwin and K. S. Sin, *Adaptive Filtering Prediction and Control* (Prentice-Hall, Englewood Cliffs, NJ, 1984), pp. 68–74.
[23] S. J. Elliott, I. M. Stothers, and P. A. Nelson, "A multiple error LMS algorithm and its application to the active control of sound and vibration," IEEE Trans. Acoust. Speech Signal Process **ASSP-35**, 1423–1434 (1987).
[24] S. D. Sommerfeldt, "Adaptive vibration control of vibration isolation mounts, using an LMS-based control algorithm," Ph.D. thesis, The Pennsylvania State University, University Park, PA (1989), pp. 84–86.
[25] S. D. Sommerfeldt, "Adaptive vibration control of vibration isolation mounts, using an LMS-based control algorithm," Ph.D. thesis, The Pennsylvania State University, University Park, PA (1989), pp. 86–89.
[26] J. C. Snowdon, "Vibration isolation: Use and characterization," J. Acoust. Soc. Am. **66**, 1245–1274 (1979).
[27] S. Timoshenko, *Strength of Materials, Part 1* (Van Nostrand, Princeton, 1958), pp. 378–381.
[28] S. D. Sommerfeldt, "Adaptive vibration control of vibration isolation mounts, using an LMS-based control algorithm," Ph.D. thesis, The Pennsylvania State University, University Park, PA (1989), pp. 118–124.

Redistribution subject to ASA license or copyright; see http://acousticalsociety.org/content/terms. Download to IP: 128.187.97.22 On: Tue, 01 Apr 2014 19:15:00